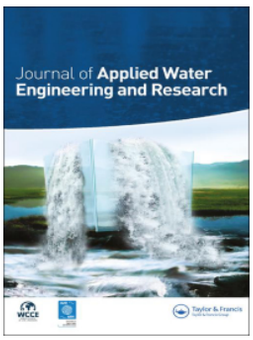

Journal of Applied Water Engineering and Research

ISSN: (Print) (Online) Journal homepage: https://www.tandfonline.com/loi/tjaw20

Effects of toe configuration on throughflow properties of rockfill dams

Geir H. Kiplesund, Ganesh H. R. Ravindra, Marius M. Rokstad & Fjóla G. Sigtryggsdóttir

To cite this article: Geir H. Kiplesund, Ganesh H. R. Ravindra, Marius M. Rokstad & Fjóla G. Sigtryggsdóttir (2021) Effects of toe configuration on throughflow properties of rockfill dams, Journal of Applied Water Engineering and Research, 9:4, 277-292, DOI: 10.1080/23249676.2021.1884615

To link to this article: https://doi.org/10.1080/23249676.2021.1884615

Journal of Applied Water Engineering and Research, 2021
Vol. 9, No. 4, 277–292, https://doi.org/10.1080/23249676.2021.1884615

Effects of toe configuration on throughflow properties of rockfill dams

Geir H. Kiplesund *, Ganesh H. R. Ravindra, Marius M. Rokstad and Fjóla G. Sigtryggsdóttir

Department of Civil and Environmental Engineering, Norwegian University of Science and Technology, Trondheim, Norway

(*Received 6 April 2020; accepted 21 January 2021*)

Rockfill dams must be equipped with defence mechanisms to counteract the destabilizing effects of throughflow forces under accidental leakage scenarios. A key component of the rockfill dam overtopping system is the rockfill dam toe, constructed in tandem with the downstream rockfill shoulder. Quantitative descriptions of effects of different toe configurations on throughflow hydraulic properties of rockfill dams are currently unavailable in international literature. To address this, experimental investigations were conducted on 1 m high model rockfill dams with disparate toe configurations. Investigation outcomes describe the effects of internal, external and combined toe configurations on pore-pressure distributions within rockfill dam models subjected to throughflow conditions. Research outcomes provide vital information which can facilitate effective decision-making with regards to rockfill dam design. The accumulated data sets could also enable development, calibration and validation of numerical design tools and dam breach models.

1. Introduction

A substantial number of the world's dams are built of rockfill and thus important to understand how best to protect these dams from catastrophic failures. Rockfill dams are vulnerable to extreme flood events leading to accidental overtopping of the dam core or even the dam crest as the dam structure is primarily composed of pervious and erodible material (Ravindra et al. 2019). Under such unanticipated scenarios, dam failure could result as a consequence of primarily three failure modes, (a) internal erosion, (b) surface erosion and (c) mass slope instability (Morán 2015). Under throughflow scenarios, highly turbulent flow entering the downstream embankment structure may develop high seepage velocities leading to transport of fine material downstream. This may lead to internal erosion if filter criteria are not fulfilled (e.g. Ravindra et al. 2018 and Morán 2015). Further, overtopping of the dam crest resulting in skimming flow over the downstream slope could lead to progressive surface erosion (e.g. Hiller et al. 2018 and Abt and Johnson 1991). Moreover, an internal build-up of dynamic pore pressures under such extreme scenarios may trigger mass slope instability and sliding (Morán 2015 and Morán and Toledo 2011).

Effective design of safe rockfill dam structures requires an understanding of the behaviour of rockfill dams exposed to throughflow and overflow scenarios. Ability to predict and model flow through rockfill dams can facilitate effective design and dam safety assessment. Past theoretical, numerical, and experimental studies have made attempts at quantitatively describing flow through and stability aspects of rockfill dams exposed to extreme scenarios. Experimental studies such as by Javadi and Mahdi (2014), Siddiqua et al. (2013), and Hansen et al. (1995a, 1995b) have investigated model rockfill dams subjected to throughflow and overflow conditions. The underlying objective of these studies was to quantitatively describe and predict initiation and progression of failure in rockfill dams from hydraulic and geotechnical standpoints. Numerical and theoretical investigations, such as by Larese et al. (2015), Hansen and Roshanfekr (2012), Hansen et al. (2005), Worman (1993), and Townsend et al. (1991), have made attempts at development and validation of empirical methodologies and numerical tools, for modelling behaviour of rockfill embankments subjected to extreme throughflow and or overtopping conditions.

Additionally, past studies by Morán et al. (2019), Javadi and Mahdi (2014), Siddiqua et al. (2013), Cruz et al. (2009), Marulanda and Pinto (2000), Solvik (1991) and Leps (1979) have stated that the toe section of rockfill dams could be a critical location for failure initiation under throughflow scenarios. Turbulent seepage flow is discharged through a relatively small cross-sectional area at the flow exit zone leading to convergence of streamlines. The generated dynamic drag and lift flow forces may lead to the removal of material at the toe section. Progression of such unravelling erosion in the upstream direction results in deep-seated slides further destabilizing the downstream embankment structure (Leps 1979). This effect is compounded while dealing with rockfill dam structures built with narrow-steep abutment profiles (Figure 1).

*Corresponding author. Email: Geir H. Kiplesund geir.h.kiplesund@ntnu.no

Figure 1. Downstream face of dam Svartevatn, Norway, built with narrow-steep abutment profiles (Photo P.H. Hiller, NTNU).

Ripraps comprising of large natural rock elements are employed in rockfill dams to protect the downstream slopes against erosion due to leakage or overtopping (Hiller et al. 2019 and Toledo et al. 2015). Further, rockfill dam toes are commonly coupled with the downstream rockfill dam structure to control seepage flow in the zone where it exits the dam. Rockfill dam toes may also be designed to counteract the destabilizing effects of accidental seepage flows entering the downstream dam structure. Internal, combined, and external toe configurations are commonly encountered in rockfill dam engineering. The internal downstream toe, generally constructed employing coarse rockfill, forms a high permeability region. Thus, the toe facilitates efficient drainage of seepage water away from the dam structure and thereby regulates the internal pore pressure build-up in accidental situations. The external toe configuration is constructed on the toe sections of existing rockfill dams to provide added stability at the seepage exit face under accidental leakage scenarios (e.g. Morán et al. 2019 and Morán 2015).

Over the past several decades, a considerable number of studies have focused on better understanding the stability aspects of ripraps under overtopping conditions. Contributions in this regard have been made by studies such as Ravindra et al. (2020), Hiller et al. (2018), Peirson et al. (2008), Dornack (2001), Chang (1998), Frizeii et al. (1998), Sommer (1997), Abt and Johnson (1991), Larsen et al. (1986), Knauss (1979), and Olivier (1967). However, few past experimental studies have investigated the behaviour of rockfill dams with toe structures under extreme scenarios. In this regard, recent studies such as Morán et al. (2019) and Morán and Toledo (2011) have conducted experimental studies on rockfill dam models with external rockfill toes. This was to document the hydraulic and geotechnical effects of an external toe on the performance of rockfill dams under extreme situations. This research also led to the development and further validation of a design methodology for external toes for rockfill dams. Apart from the present study looking at the efficacy of external toes, experimental studies focusing on investigating the behaviour of rockfill dams constructed with disparate toe configurations is currently unavailable in international literature.

However, as previously outlined, rockfill dam toe structures play a key part in stabilizing the embankment structure under overtopping scenarios. Hence, it is of significance to comprehend the effects of various toe configurations on throughflow properties of rockfill dams under extreme loading scenarios. Generation of knowledge in this regard can facilitate effective design and construction of these structures. This could also enable further development and validation of numerical design tools and dam breach models. This article presents findings from experimental model studies conducted on 1 m high rockfill dam models with disparate toe configurations. The rockfill dam models are conceptual laboratory cases built for comparison of selected toe configurations considering the study objective. The objective of the study is to obtain qualitative and quantitative descriptions of effects of toe configurations on throughflow hydraulic properties of rockfill dams.

2. Experimental setup and testing program

2.1. *Physical model description*

The model studies were conducted in a flume (25 m long, 2 m deep and 1 m wide) at the hydraulic laboratory of NTNU, Trondheim (Figure 2). Discharge to the flume was supplied by pumps with a combined capacity of $Q = 0.4$ $m^3\ s^{-1}$. A SIEMENS SITRANS Mag 5000 discharge meter with a flow rate measurement accuracy of $\pm$ 0.4% was used. The basic model setup comprised of the downstream half of a 1:10 scale rockfill dam structure of height $H_d = 1$ m, bottom width $B_b = 1.8$ m, top width $B_t = 0.3$ m (Figure 3(a)) and transverse length $L_d = 1$ m. The size of the model is primarily determined by the dimensions of the flume, the scale was chosen based on previous tests in the flume on riprap where it was considered desirable to have the same scale on the new model to facilitate comparison between the model setups. Choice of scale in this earlier research is discussed in Hiller et al. (2009, 2018). The scale is primarily chosen based on practical considerations. A practical size for riprap stones for manual placement was chosen with a $d_{50} = 65$ mm, compared to the riprap stone size of Norwegian rockfill dams the geometric model scale is approximately 1:10. This scale has been adopted for all subsequent model tests along this chain of research projects to facilitate comparison of results and is also adopted in new models currently under testing. The downstream embankment slope was chosen to be $S = 1{:}1.5$ (H:V) complying with Norwegian rockfill dam construction practice (Hyllestad et al. 2012). The impervious steel element incorporated in the model setup encompassed the dimensioning of the central core and the adjacent filter zones (zone (B),

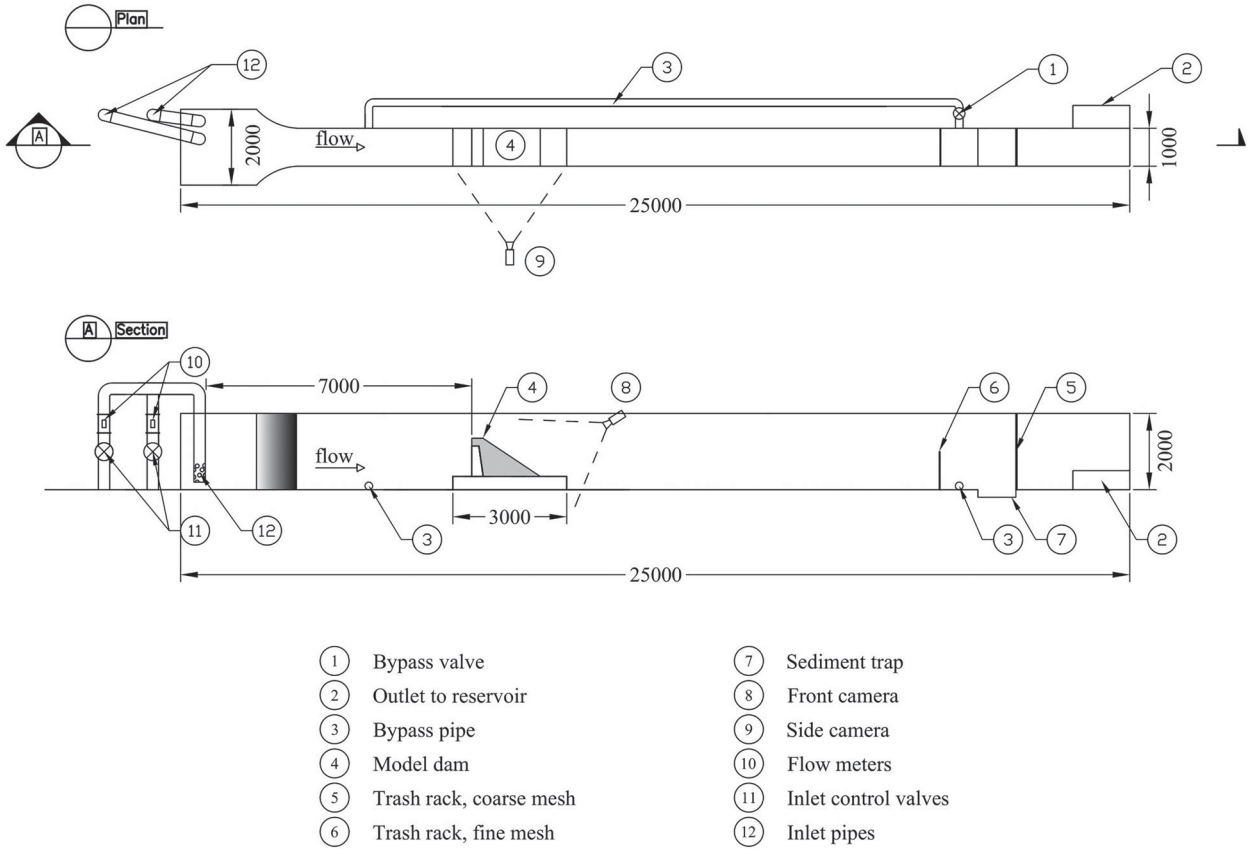

Figure 2. Layout of the flume setup present at the hydraulic laboratory of NTNU, Trondheim. (Figure by Unnar Númi Almarsson and Ganesh H.R. Ravindra).

Figure 3(b)). This is because flow through the core, as well as the adjacent sand filter zone can always be viewed as laminar. Even for large rockfill dams, flow through these zones is insignificant considering the stability of the downstream structure (Solvik 1991). Since the objective of the experimental study was to investigate the behaviour of the downstream structure of rockfill dams simulating overtopping of the dam core, an impervious element representing the central core and filter zones was incorporated to simplify model design. The thickness of the dam crest i.e. the vertical distance between the top of the impervious core-filter element and the dam crown was set as 0.2 m. This was an important parameter in the model setup and was based on the recommendations in Hyllestad et al. (2012) where, for rockfill dams with a central moraine core, a minimum of 2 metres of frost safe material is required above the core.

Basing on a study of design and constructional aspects of several Norwegian rockfill dams, three discreet rockfill dam toe structures designs were identified, namely the external, internal and combined toe configurations. Design details for over 30 Norwegian rockfill dams were obtained through the large-scale field survey conducted by Hiller (2016). Fjellhaugvatn is a 52 m high and 73 m long rockfill dam situated in Kvinnherad, Norway and the dam is equipped with an internal toe structure. The Akersvass dam is a 53 m high and 485 m long rockfill dam situated in Rana, Norway and is equipped with an external dam toe. Further, Skjerjevatn main dam constructed in Masfjord, Norway is a 30 m high and 266 m long rockfill dam provided with a combined dam toe. The majority of the investigated rockfill dam structures were provided with toe structures belonging to one of the three aforementioned categories. Hence, the experimental model setup for the present study was designed adopting these three disparate toe configurations. The dam models are conceptual and so are the different toe configurations.

Within the present study, the external toe configuration represents a trapezoidal rockfill structure constructed on the downstream slope covering the toe zone (zone (F), Figure 3(b)). The internal toe configuration is characterized by a triangular section within the downstream embankment structure comprising of coarse rockfill material (zone (E), Figure 3(b)). The combined trapezoidal toe configuration represents a coupling of the internal and external toe configurations (zone (E) + (F), Figure 3(b)). The height of the toe structure, $H_t = 0.25$ m, for the external toe configuration considered the exit zone of the no toe dam. It was further decided to have the same height for all the toe configurations. Additionally, the chosen height of the

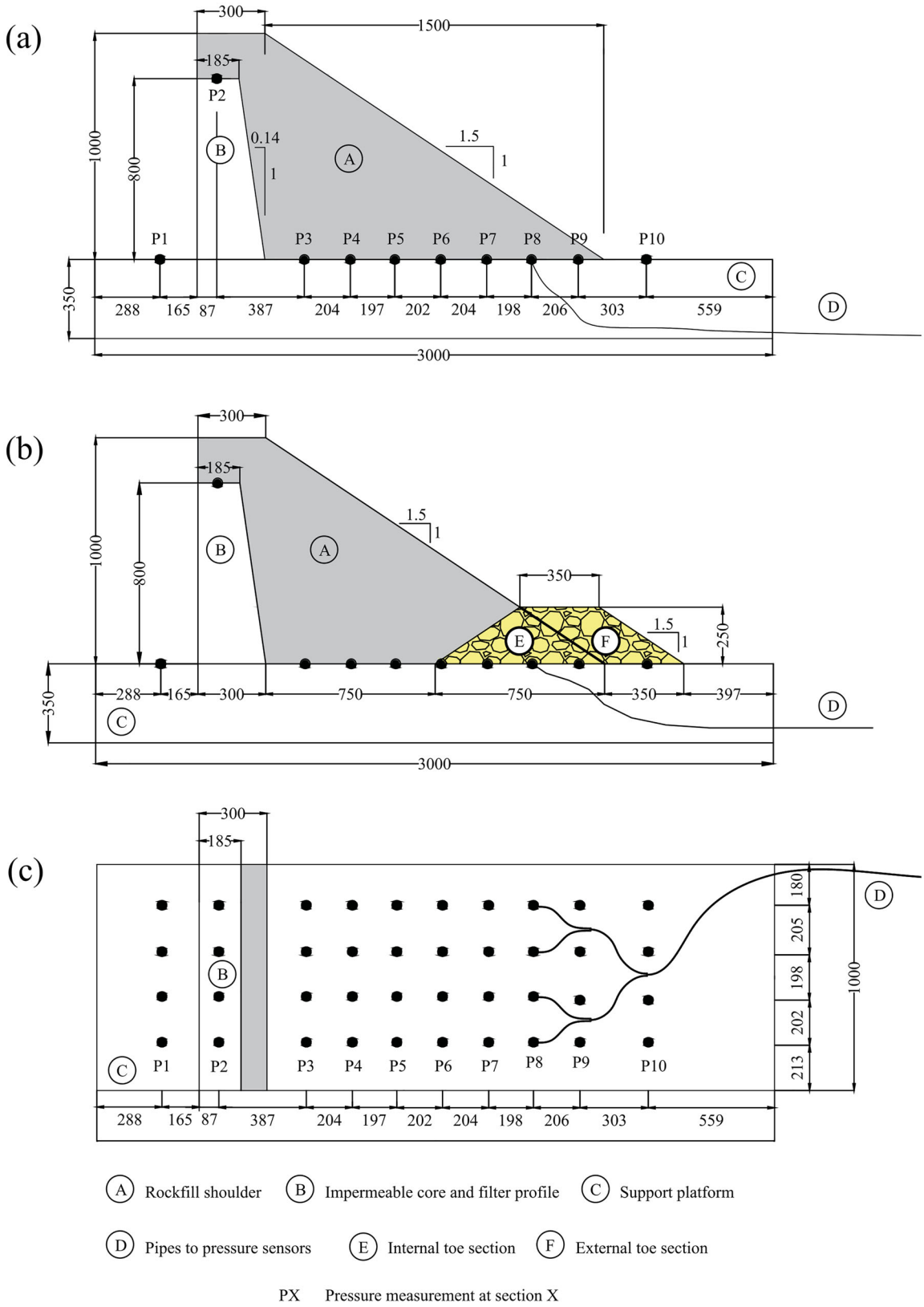

Figure 3. Depictions of the experimental setup with (a) sectional view of the rockfill dam model, (b) details regarding the disparate toe configurations and (c) planar view of the horizontal platform. (Figure adopted from Ravindra 2020).

toe structures, $H_t = 0.25$ m, was supported by a literature review of the design of several existing Norwegian rockfill dams presented within Hiller (2016). The internal toe represents an equilateral triangle with altitude H_t. The external toe dimensions were so chosen partly as to achieve a similar volume of construction as compared to the internal toe, but also to allow for sufficient length downstream of the dam structure for complete flow development. Multiple other dam toe configurations could have been chosen but these were considered appropriate for the objectives of this study in the framework of conceptual experimental models.

The rockfill dam models were constructed on a horizontal support platform of length 3 m, width 1 m and height 0.35 m. This was to elevate the entire test setup from the flume bottom to avoid backwater effects (Figure 3). The experimental setup was situated sufficiently downstream of the inflow section of the flume to achieve calm flow upstream of the test models (Figure 2). A series of 10 pressure sensors (P1-P10) were coupled with the experimental setup for measurements of internal pore pressure developments at different locations at the base of the dam structure as shown in Figure 3(a) and also for monitoring of the upstream/downstream water levels during the overtopping tests. The pressure sensors were connected to the platform through a pipe network linked to an array of holes as depicted in Figure 3(c). A series of four holes were provided along the width of the platform at each spressure measurement location for measurement of the average pressure levels and as a safety precaution against blockage. Two SIEMENS SITRANS P210, 0–250 mb pressure sensors were employed at locations P1 and P2 and eight SIEMENS SITRANS P210, 0–160 mb sensors were used at locations P3 to P10. These sensors provide reliable performance with high accuracy of 0.25% of the full-scale value, which translates to ± 0.6 cm for P1 and P2 and ± 0.4 cm for P3-P10. Depiction of the model setups from the laboratory is presented in Figure 4. Figure 4(b–d) presents respectively the external, internal, and combined toe configurations. Conversely, Figure 4(a) depicts a homogeneous dam, that is referred to as with 'no toe', to reflect that the material in the toe (zone E), is the same as in the shell (zone A).

The dam shoulder comprised of well-graded rockfill material of density $\rho_S = 2720\,\text{kg m}^{-3}$, median particle size $d_{50,S} = 0.0065$ m, coefficient of uniformity of $C_{u,S} = 7.5$ and porosity of $n = 0.35$. The toe sections were constructed employing uniformly graded coarse rockfill of density $\rho_T = 2860\,\text{kg m}^{-3}$, median stone size $d_{50,T} = 0.052$ m, coefficient of uniformity $C_{u,T} = 1.42$ and porosity of $n = 0.51$ (Lev and Anantharamu 2020). The grain size distributions for the rockfill shoulder and the toe material are presented in Figure 5. The material gradations were scaled down from a database of gradation curves from large-scale rockfill dam constructions with a scaling ratio of 1:10. Figure 6 presents the upper and

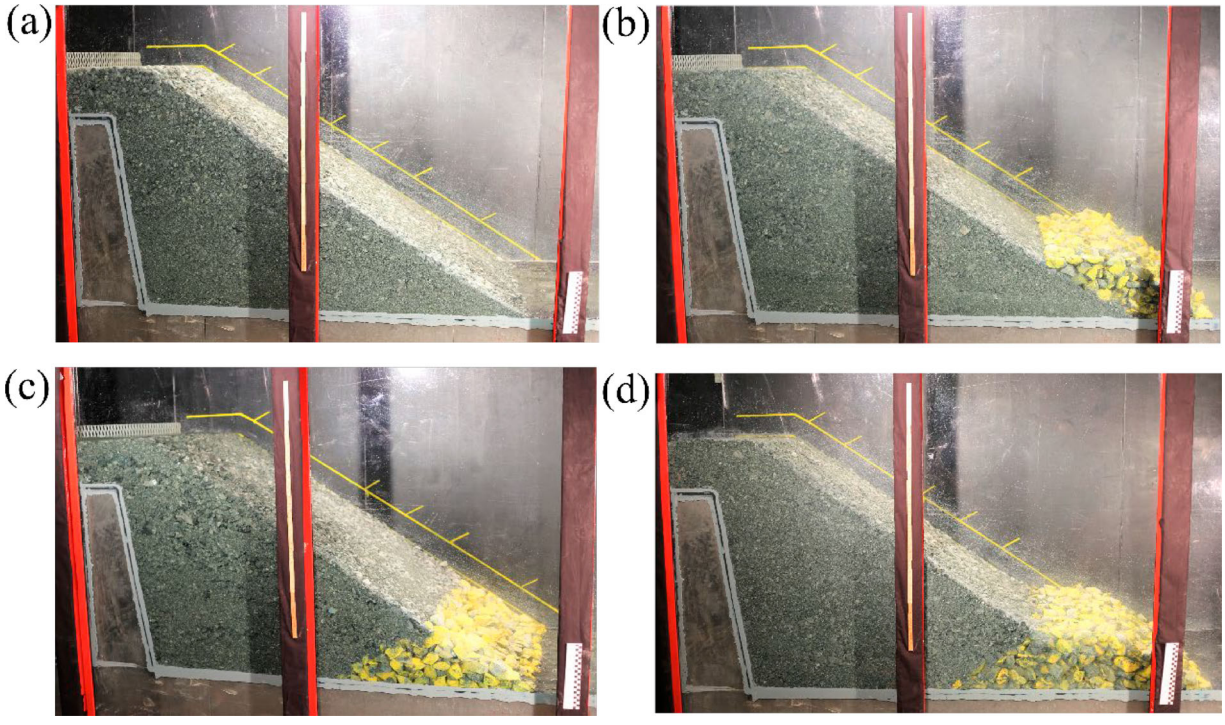

Figure 4. Depictions of the rockfill dams with (a) no toe, (b) external toe, (c) internal toe and (d) combined toe configurations (Figure adopted from Ravindra 2020).

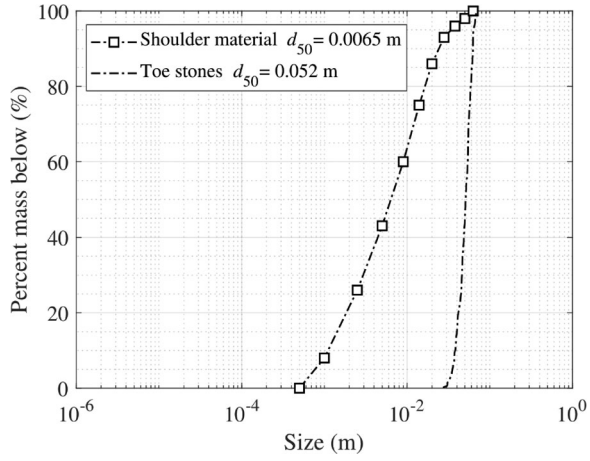

Figure 5. .#Grain size distribution curves for the rockfill shoulder and toe material (both at model scale).

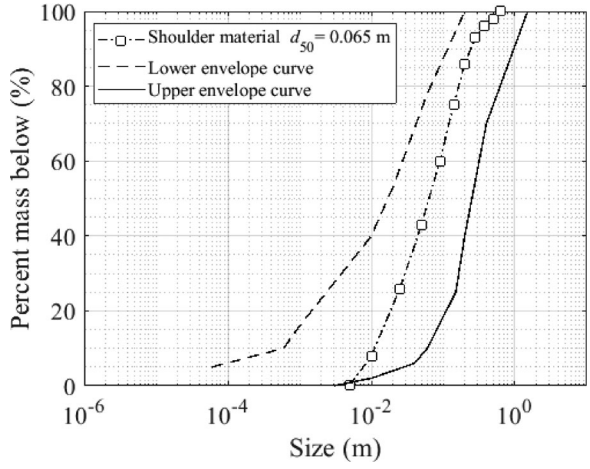

Figure 6. .#Grain size distribution enveloping curves (scaled 1:10) from dam database and for chosen shoulder material (unscaled).

lower boundary envelopes for the database of dams used for obtaining the sizing of the rockfill shoulder material. The database comprised of Norwegian dams such as Strandevatn, Aura, Skjellingavatn, Homstøl, Tunsbergdalen and so on (NTNU 2020). However, as can be inferred from Figure 6, the gradation was biased towards the coarser range of the database. This was due to restrictions with the pumping systems installed in the laboratory, inclusion of very fine particles $<$ 0.5 mm was not possible in the model. Hence, the gradation was carried out with 0.5 mm as the minimum allowed particle size.

The gradation curve for the rockfill shoulder material was also evaluated against the filter criteria recommendations detailed within the national dam safety guidelines (Hyllestad et al. 2012). The guidelines offered by the NVE are based on the criteria outlined by the USDA (2017). The NVE defines a base core material, sampled as the most commonly found moraine soil types in Norway. Based on the base gradation for the core material (d), the design curve limits for the transition zone (D) between the core and the rockfill shoulder can be arrived at as $D_{15,\min} = 4{\cdot}d_{15}$, $D_{15,\max} = 5{\cdot}D_{15,\min}$ and a uniformity coefficient $C_u = D_{60}/D_{10} > 5$. Further, the obtained gradation curve for the transition zone can be employed to compute the boundaries for the rockfill shoulder material using the criteria, $4 < D_{15}/d_{15} < 40$, $D_{50}/d_{50} < 25$ with $C_u = D_{60}/D_{10} > 6$. The gradation curve for the rockfill shoulder material (Figure 6) was found to satisfy these guidelines for autostability.

The rockfill dam shoulder was built in layers of 0.1 m and was hand compacted using a 0.2 m x 0.2 m tamper weighing 4.54 kg. The primary goal with regards to compaction effort was to achieve reproducibility, not to replicate in scale a specific compaction energy. That is, adopt a specific compaction strategy so that the same compaction effort is implemented throughout the testing program. As a standard method of construction, the tamper was dropped free from a vertical distance of 0.1 m for 10 tampings at each location to achieve uniform energy of compaction over the entire experimental testing program. The toe sections were constructed by manual placement of stones and were further hand compacted to avoid large voids in the structure.

2.2. *Testing methodology*

The study objective was to provide qualitative and quantitative descriptions of hydraulic responses of the dam structures with different toe configurations exposed to incremental throughflow levels. To accomplish these tasks, the rockfill dam models were subjected to incremental levels of overtopping in regular discharge intervals of $\Delta q = 0.5{\cdot}10^{-3}$ m^3 s^{-1} commencing at $q_i = 1{\cdot}10^{-3}$ m^3 s^{-1} for N discharge steps. The discharge levels were maintained constant over regular time periods of $\Delta t = 1800$ s to allow for flow stabilization at each overtopping interval. The intervals were however not sufficiently long to allow for a completely steady-state flow to develop. To analyse the development of throughflow patterns, the pore pressure levels at the base of the dam structure were recorded at various locations employing the pressure sensor- data logger setup at an acquisition rate of 100 Hz. Further, high-quality images and videos of the tests were acquired (Figure 2). The procedure was repeated until the discharge was large enough to cause erosion of the crest to reach the metal core. The critical applied discharge magnitude giving rise to initiation of complete erosion of the dam crest is represented as q_c.

3. Data analysis

The experimental study yielded time series of pore pressure measurements at each sensor location (Figure 3), corresponding to each discharge level, as illustrated in Figure

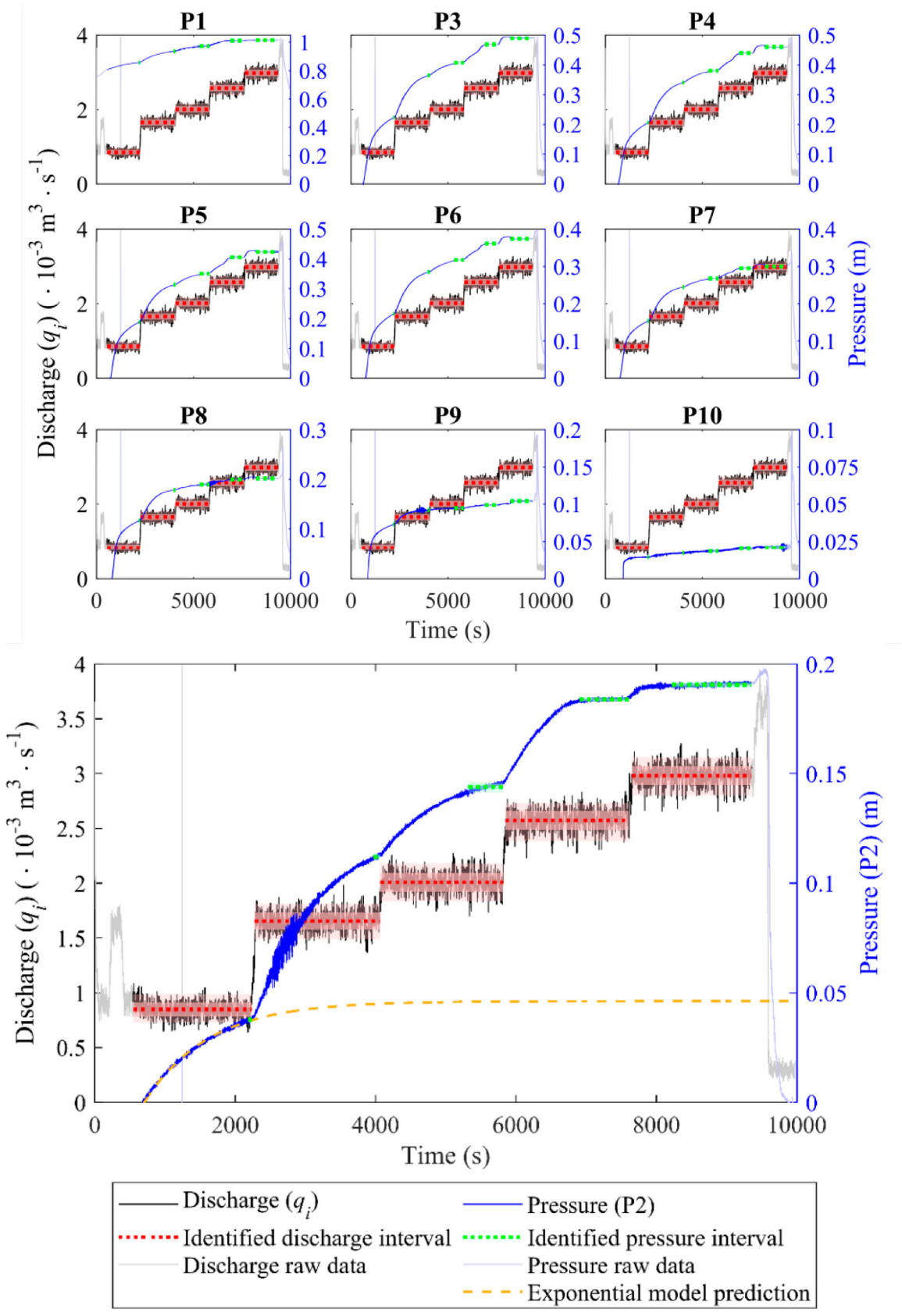

Figure 7. Selection of representative pressures for various discharge magnitudes.

Table 1. Descriptions of toe configurations, testing methodology and critical discharges (Ravindra 2020).

Test no.	Toe configuration	q_i (10^{-3} m^3 s^{-1})	N (–)	Δt (s)	q_c (10^{-3} m^3 s^{-1})
1	No toe	1.0–3.5	6	1800	3.5
2	No toe	1.0–3.0	5	1800	3.0
3	No toe	1.0–5.0	9	1800	5.0
4	External	1.0–3.5	6	1800	3.5
5	External	1.0–5.5	10	1800	5.5
6	External	1.0–5.0	9	1800	5.0
7	Internal	1.0–4.0	7	1800	4.0
8	Internal	1.0–5.0	9	1800	5.0
9	Internal	1.0–4.5	8	1800	4.5
10	Combined	1.0–4.0	7	1800	4.0
11	Combined	1.0–3.0	5	1800	3.0
12	Combined	1.0–3.0	5	1800	3.0

7 for test 1 from Table 1. The plot depicts development of pore pressures at sensor location P2 (Figure 3) as a function of the applied discharge magnitude (q_i). As can be observed from the depictions, considerable variability and fluctuations were found in the data sets owing to the nature of the experimental setup. Dynamic pore pressures generated within the dam structure during throughflow exposure lead to noise in the collected raw datasets.

The pore-pressure development trend presented in Figure 7 also shows that the pressure magnitudes at different applied discharge levels undergo increments with time to attain steady state flow conditions. Considering the variability in the raw datasets and the time-lag in the pore pressure response, it was necessary to perform statistical analyses in order to obtain representative magnitudes for (1) applied discharge magnitudes and (2) pore-pressures at different locations within the dam structures for the respective applied discharge magnitudes.

A mean value change point analysis was performed in order to calculate representative values for the discharge levels, filter out inconsistencies and transition zones in the discharge signal (e.g. where the increase from one discharge level to the next has been slow), and identify the time intervals for each discharge level. The change point analysis resulted in a set of discharge levels with corresponding mean, median, variance statistics, 95-percentile values, and time intervals.

In order to obtain representative pore pressure values for each identified discharge level, one must consider that the pore pressure is not stationary for the entire time interval of the discharge level, as the pore pressure builds up gradually after a discharge level increases. The average pore pressure registered in the time interval of one discharge level is therefore not a representative value of the equilibrium pore pressure. Conversely, using the last registered or the maximum value in the time interval is also not advisable, since there is variability in the pore pressure raw data. The challenge is thus to identify a time series for the pore pressure data, which is stable enough to be considered close to stationary, but large enough to be considered representative.

To achieve this, the following approach was taken. For a given discharge level q_i occurring on the time interval $[t_{i,1}, t_{i,2}]$, the coefficient of variation ($c_{v,i,x,t}$) divided by the square root of the number of samples ($m_{i,t}{}^{1/2}$) was calculated for each pressure sensor x, and time interval $[t, t_{i,2}]$ for all $t_{i,1} \leq t \leq t_{i,2}$. Then the time at which the sum of the coefficients of variation for all the pressure sensors divided by the square root of the number of samples in the interval $[t, t_{i,2}]$ is minimized (t_{min}) was identified, and the pore pressure measurements in the interval $[t_{min}, t_{i,2}]$ were used to calculate the representative value for the pore pressure of each sensor for the given discharge level:

$$t_{\min} = \min\left(\sum_{\forall x} c_{v,i,x,t}/m_{i,tt}{}^{1/2} \forall t_{i,1} \leq t \leq t_{i,2}\right) \quad (1)$$

$$P_{\text{mean},i,x} = \left(\sum P_{x,t}, \forall t_{\min} \leq t \leq t_{i,2}\right)/m_{i,t\min} \quad (2)$$

The coefficient of variation divided by the square root of the number of samples tends to decrease as the number of samples increase when the sample distribution is stationary, but increases when one is moving out of the stationary region of the signal. Hence, this metric is able to identify a trade-off point between sufficient sample size for representativeness without veering into the non-stationary region of the signal.

The statistical analysis of the raw data resulted in representative values and statistics for the discharge levels, with corresponding pore pressures for each location and discharge level.

Owing to practical restrictions associated with carrying out the tests, it was necessary to limit the timeframe for each test that was undertaken with a limited time interval for each discharge level. This means that the risk exists that steady state was not achieved for the pore pressure in every test. To verify whether or not the pore pressure measurements had achieved equilibrium, an exponential regression and extrapolation routine was made, in which the pore pressure measurements within each discharge time interval $[t_{i,1}, t_{i,2}]$ was fitted to an exponential model: $P_{pred,i}(t) = C + A{\cdot}\exp[-B{\cdot}(t–t_{i,1})]$, where A, B and C are

regression coefficients. By extrapolating this model so that t reaches infinity, one obtains a model prediction for the value of the pore pressure ($P_{pred,i}(t_\infty) = C$) if the discharge level had been maintained at the same level for a long time. By comparing this prediction with the calculated pressure value, one could assess if there was reason to suspect that steady state had not been achieved. It was found that the predicted value rarely was more than 15% larger than the calculated value, from this one can conclude that a steady state was not always reached. However, the deviations are quite small when considering that the researchers are primarily looking at relative differences between various geometries and are not focusing on absolute values of pore pressure. Based on this the uncorrected data are considered accurate enough to derive relative differences.

4. Experimental results

4.1. Pore pressures and phreatic surface developments

As described previously, pore pressures were recorded at 10 sensor locations as functions of applied discharge magnitudes. The raw datasets were further subjected to the change-point based statistical analysis detailed earlier. The analysis resulted in 10 pore pressure values (P1-P10) for each applied discharge magnitude. Figure 8 shows the pore pressure development at different locations for Test 1 (Table 1) conducted with no toe. The pore pressure values for the respective discharge magnitudes represent the stable, representative values attained after maintaining the discharge magnitude at the respective levels over time periods of $\Delta t = 1800$ s. In Figure 7, P1 shows the upstream still water level, P2 represents the pore pressure above the impermeable core, P3 to P9 depict pore pressures within the downstream supporting rockfill, and finally, P10 displays the pore pressure downstream of the dam structure.

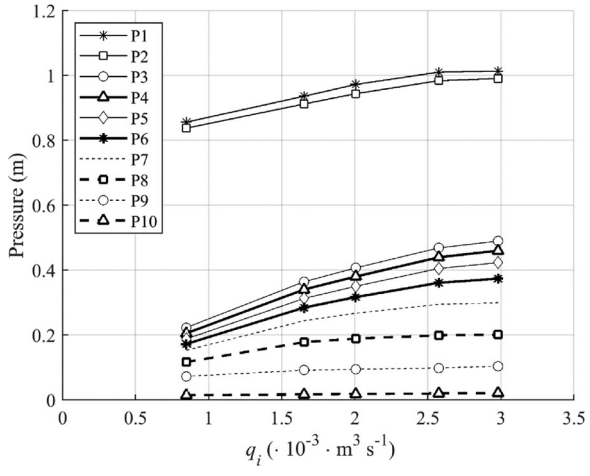

Figure 8. Pressure measurements for Test 1 from Table 1 (Figure adopted from Ravindra 2020).

As can be observed from Figure 8, the individual pore pressure levels within the supporting fill were found to undergo non-linear increments as functions of the applied throughflow magnitudes for Test 1. The non-linear trends in pore pressure developments were found to be less pronounced at the downstream section of the dam structure. Similar trends were observed for all the tests. The observed non-linear trends in pore-pressures present an important opportunity with regards to scaling of the test results. The present rockfill dam model was designed based on Froude similarity adopting a scaling ratio of 1:10. Flow conditions at prototype scales would always be non-linear or fully turbulent owing to the sizing of the rockfill material. To enable scaling of test results from the model scale to the prototype scale, it is of essence to ensure non-linear flow conditions also at the model scale. Results from Figure 8 validate that flow conditions were non-linear in nature thereby permitting Froude scaling.

This statistical methodology was further employed to obtain representative pore pressure values at different locations for the different applied discharges for all the tests presented in Table 1. Discharges for the tests were in the interval $1{\cdot}10^{-3\text{–}4}{\cdot}10^{-3}$ m^{3}s^{-1} with steps of $\Delta q = 0.5{\cdot}10^{-3}$ m^{3}s^{-1}. Since the primary focus of the study is to comprehend throughflow aspects of rockfill dams, the maximum flow considered for the analyses was limited to $4{\cdot}10^{-3}$ m^{3}s^{-1} as higher discharge levels were observed to constitute surface flow. In other words, in general, applied discharge magnitudes $> 4{\cdot}10^{-3}$ m^{3}s^{-1} were found to give rise to overtopping of the dam crest section.

The effects of different toe geometries on pore pressure and phreatic surface developments within the rockfill dam structures were investigated. Figure 8 shows the average pore pressure development trends within the disparate tested dam structures (Table 1) represented for the respective throughflow magnitudes (q_i). P10 represents the water level downstream of the dam for setups (a) no toe and (c) internal toe and signifies pore-pressures within the external toe for setups (b) external toe and (d) combined toe.

As can be observed from Figure 8, the flow patterns upstream of sensor location P3 were found to be consistent across models. During the tests, the water surface profiles upstream of the dam crest section (P1) were observed to be horizontal in nature as they entered the crest. This suggests that there are negligible energy losses between pressure sensor location P1 and the dam crest, this is expected as the average velocity in the cross-section is around $4{\cdot}10^{-3}$ m$\cdot$s^{-1}, and $2{\cdot}10^{-2}$ m$\cdot$s^{-1} at the entry to the crest. There is also a small entrance loss due to the flow contraction and grate holding back the crest material that we have not corrected for in the figures as it is in the magnitude of $1{\cdot}10^{-5}$ m. Hence in Figure 8, the water surface profiles are shown as extensions of pressure measurements from P1 onto the entry surface of the crest using horizontal lines, between the entry section and P2 a linear interpolation is assumed.

Downstream of P2 no pressure profile is drawn as the flow was found to undergo transitions over the core-filter element and in turn plunged into the downstream dam structure towards P3. The plunge patterns were visually observed during the experiments to be near vertical drops. This could be explained as being a consequence of the steep slope of the core-filter element. A milder slope would lead to more moderate flow patterns. No clearly defined phreatic surface profiles could be identified within this flow reach as the water is percolating down as unsaturated flow upon traversing over the edge of the impervious core-filter element.

Further, for rockfill dam structures with no toe (Figure 9(a)) and with external toe (Figure 9(b)), pore pressure profiles closely resembling smooth non-linear pore pressure profiles were observed within the rockfill shoulders. The pore-pressure development profiles were found to be correlated with the applied throughflow magnitudes (q_i). The spacing between the pore pressure profiles were found to undergo decrements with incremental overtopping, owing to the non-linear nature of pore-pressure developments at each of the sensor locations (Figure 8). From preliminary visual observations of Figure 9, the external toe configuration was seen to have minor impacts on throughflow development within the rockfill shoulder. Further, due to the highly porous nature of the toe material, the flow downstream of the shoulder was found to be affected to a minor degree by the external toe configuration. The primary difference in behaviour of the two structures was the additional protection offered by the external toe against scouring and erosion at the seepage exit face. Damage was observed at the exit face on the rockfill shoulders of the models constructed without toes (referred to herein as the 'no toe' model). This was due to surface erosion resulting as a consequence of the drag forces generated over the seepage exit face and due to the occurrence of occasional slides leading to scouring. However, no such damages were observed for dams constructed with an external toe.

For dam models built with internal (Figure 9(c)) and combined (Figure 9(d)) toe configurations, significantly different pore pressure development profiles were obtained as juxtaposed with the dam models built with external toe and with no toe. The pore pressures experienced much steeper drops from P3 moving downstream towards P6 (Figure 9) because of a high permeability in the internal toe reaches. The pore-pressure magnitudes downstream of P6 were further seen to experience mild progressive reductions within the toe structures finally exiting the dam structure. The throughflow development patterns within the dam structures constructed with internal and combined toes could be seen to closely resemble each other, entailing minimal effects of the external reach of the combined toe structure on throughflow. No damage to the toe zones were observed for either of the toe configurations even at maximum throughflow magnitude.

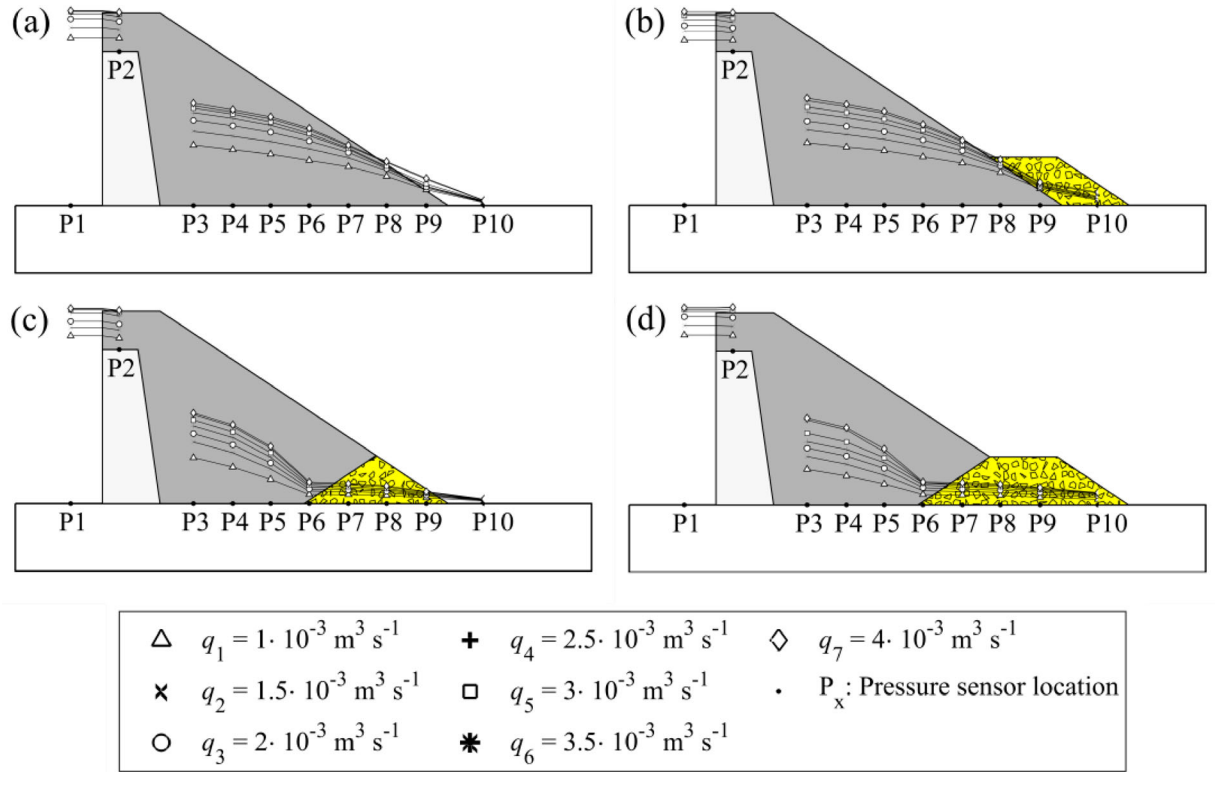

Figure 9. Pressure development within the tested model rockfill structures with (a) no toe, (b) external toe, (c) internal toe and (d) combined toe configurations (Table 1) subjected to incremental throughflows (q_i) (Figure modified from Ravindra 2020).

Table 2. Per cent change in pressures relative to dam with no toe.

Toe type	$q_i(10^{-3}$ m^3 s$^{-1})$	P2 (%)	P3 (%)	P4 (%)	P5 (%)	P6 (%)	P7 (%)	P8 (%)	P9 (%)
External	1	– 1	3	4	7	8	9	12	4
	1.5	– 2	2	2	3	4	5	7	3
	2	– 4	– 1	– 1	1	1	3	6	1
	2.5	– 3	0	1	2	3	5	8	2
	3	– 2	1	2	3	4	6	7	– 4
	3.5	– 1	5	6	6	5	8	4	– 16
	4	0	5	5	6	5	8	4	– 15
Internal	1	– 1	– 24	– 34	– 53	– 80	– 77	– 73	–64
	1.5	– 1	– 17	– 26	– 46	– 78	– 75	– 69	– 57
	2	– 3	– 18	– 26	– 44	– 77	– 74	– 67	– 54
	2.5	– 1	– 16	– 24	– 42	– 76	– 72	– 64	– 51
	3	0	– 14	– 21	– 39	– 74	– 70	– 61	– 51
	3.5	0	– 11	– 18	– 36	– 73	– 68	– 61	– 56
	4	0	– 11	– 18	– 36	– 72	– 67	– 59	– 55
Combined	1	2	– 41	– 48	– 59	– 77	– 74	– 67	– 51
	1.5	2	– 35	– 41	– 53	– 75	– 72	– 64	– 40
	2	2	– 33	– 39	– 50	– 73	– 70	– 60	– 32
	2.5	2	– 32	– 36	– 47	– 71	– 68	– 56	– 26
	3	2	– 26	– 31	– 43	– 69	– 65	– 53	– 28
	3.5	3	– 15	– 20	– 39	– 71	– 64	– 54	– 37
	4	3	– 15	– 19	– 36	– 70	– 63	– 53	– 36

Table 2 shows the per cent change in pore pressures between the baseline case with no toe and the different toe geometries tested. The cells in the table are colour-coded according to per cent change in pore pressure relative to dam with no toe with 0–20% as white up to 61–80% as dark blue. These data have further been presented graphically in the form of three-dimensional plots in Figure 10. Since the analysis goal was to provide quantitative descriptions of flow through the dam shoulder structure, the upstream and downstream water level measurements P1 and P10, respectively, were excluded from the analysis.

Concerning pressure differences at P2 (Table 2), only minor deviations ($< \pm$ 4%) between the differing model setups were found. This is an expected outcome as the toe geometry does not affect flow development upstream of P3 for any of the flow conditions seen in these tests. This is due to absence of contiguous pressure flow all the way up to the top of the core, the flow is interrupted by a zone of plunging non-saturated flow just downstream of the impervious core-filter element. Due to this, the pore pressures at the top of the core are only determined by the geometry of the core and crest as well as the properties of the comprising material. The observed variability can be primarily attributed to measurement uncertainty and variations in the material properties from test to test. The main factors in this regard are the compaction process and how well the material is mixed after each test and during the construction process.

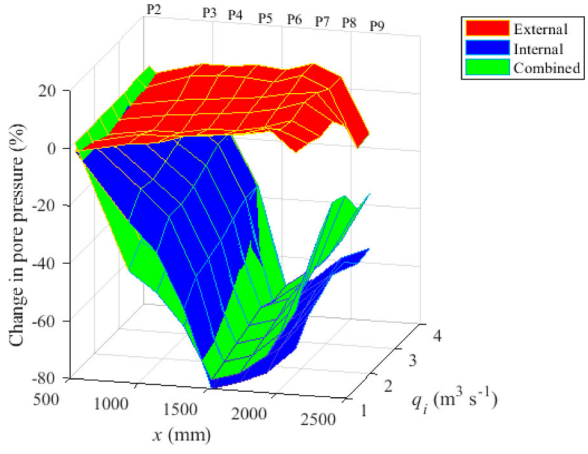

Figure 10. Per cent change in measured pressures relative to dam with no toe as a function of distance from the upstream face (x) and discharge (q_i).

For the external toe case, results from Table 2 show only marginal changes in pore pressures as compared to the dam with no toe. The pore pressure developments within the downstream supporting fill (P3-P9) of the dam, mainly at the sensors closest to the toe and at higher flows show up to 8% increase in pore pressures at P7 and P8. Adding an external toe introduces friction losses within the toe structure. This results in minor increases in the pore pressures within the supporting fill, especially towards the downstream section. At sensor P9, however, a reduction in pore pressures were observed for larger flows. A likely cause of this is erosion of the rockfill material through the external toe. Sensor P9 is located close to the transition from supporting fill to external toe and it would not take much loss of material to get a small piping causing a drop in pore pressure at some point along the pressure sensor alignment.

From Table 2, significant reductions in pore pressures were observed for the internal toe case. The greatest reductions were found at sensor P6, situated at the inner edge of the internal toe, where pore pressures are reduced by between 72 and 80%. At sensor P3 which is the first sensor downstream of the core, pore pressures were reduced by 11–24%. At the centre of the internal toe (P8), pore pressures were reduced by 59–73%. The combined toe was found to behave very similarly to the internal toe with slightly increased pore pressures at sensors P6 to P9. However, in the supporting fill at P3 to P5, the pore pressures were somewhat reduced. From a theoretical standpoint, the external portion of the combined toe configuration should result in a marginal raising of internal pore pressures as described earlier for the external toe case. However, this was not seen from the recorded data, potentially due to variability in permeability of the shoulder material. Changes in the permeability of the material could be due to inconsistencies in the mixing, placement, and compaction of materials after each test. Erosion of some supporting fill material through the toe could also affect the results, however, such erosion was not visible during the tests. These deviations from what was expected clearly illustrate the uncertainties related to material parameters in such a construction even under controlled laboratory conditions. Similar uncertainties are also to be expected at prototype scale. These issues create challenges when laboratory data is used for calibrating and verifying numerical models. Calibration of one model may not be fully valid for another model, due to variations associated with the material properties. This can be the case even for models comprising of the same material since there can still be deviations in mixing and compaction that affect the properties.

4.2. Failure initiation

Discharge levels for initiation of dam breach were recorded as part of the experimental testing program (Table 1). These represent the applied discharge magnitudes leading to surface overflow and in turn, to progressive erosion of the dam surface giving rise to complete degradation of the dam structure. Figure 11 below shows one of the models without toe after failure initiation. As a key observation, critical locations for breach initiation were always found to be situated over the upstream crest of the dam structures being independent of the flow conditions in the lower reach of the dams. This effect was due to the flow conditions over the crest being independent of the flow conditions in the lower part of the dam. The variation in failure discharge can be attributed to variations in the material properties between tests as well as irregularities in the geometry of the crest section due to construction efficiency.

None of the tested dams experienced irreversible dam breach at the toe section even with the application of maximum throughflow magnitude which could be accommodated through the crest. Significant damage in the exit zone of the throughflow on the surface of the downstream shoulder were observed for dams constructed with no toe. There was no visible erosion at the toe sections for dams with internal, external or combined toes. The entire surface of the supporting fill was not visible in these cases, but material transport was not observed in the water discharging from the dam toe. So, it could be inferred that the toe structures protected the supporting fill against erosion, even though the transition from supporting fill to toe did not entirely fulfil the filter criteria. In a full-scale dam, there would have been an additional filter layer in the transition between supporting fill and dam toe.

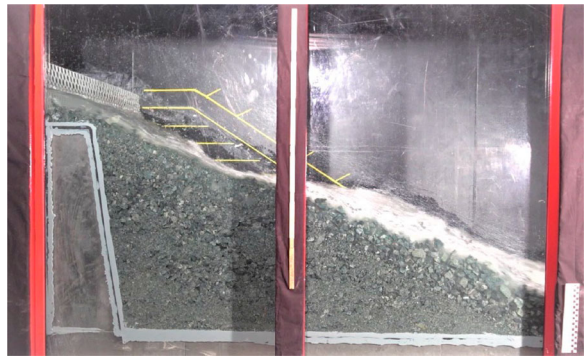

Figure 11. Image of model without toe during breach.

Furthermore, no clear correlations were found between the magnitude of maximum throughflow required for initiation of dam breach and the toe configurations employed (Table 1). This suggests that the amount of throughflow entering the dam structure is primarily dependent on properties of the dam crest such as the dimensioning and the permeability rather than on the downstream flow conditions.

5. Discussions

The research outcomes from the present study demonstrate the significant impacts the highly permeable internal and the combined toe structures can have with regards to reductions in pore pressures within the downstream supporting rockfill. Slope stability is highly affected by pore pressure within the dam structure as demonstrated by past research works such as Worman (1993) and Morán and Toledo (2011). Effective drainage of seepage flows from the dam structure leads to a more stable dam structure. Findings from this study provide evidence to show that overall stability and safety of a rockfill dam can be significantly improved by the introduction of a high permeability toe drain within the downstream embankment structure.

There are however other effects of reducing pore pressures that also need to be addressed. Amplification of the drainage capacity in the toe and lowering of the pore pressures will lead to increased void velocities within the

structure which could have negative consequences, such as increased internal erosion, if filter criteria are not sufficiently met between the different zones. No filter was incorporated at the interface between the well-graded shoulder material and the toe within this study, however, no transport of fine materials was observed downstream of the toe for any of the tested dams even with maximum permissible throughflow. Deviations from pressure profiles expected from theoretical considerations indicate that there in some cases could have been some erosion of supporting fill material through the toe material. Such erosion was however not observed during the testing. A filter within this section would, however, be more important with a supporting fill containing a greater amount of fine materials than used for these tests. Flow conditions in the downstream supporting rockfill and toe structures could be thought of as independent of the source of flow, be it flow over the top of the core or leakage through the core. This however only applies in a two-dimensional situation with equal overtopping or leakage flow per metre dam, in reality a leakage through the core would be much more concentrated and would lead to increased erosive forces compared to an overtopping of the core. Further research on investigating toe stability under catastrophic scenarios such as extreme leakage through the core due to e.g. piping is required. Furthermore, the differences in results between the internal toe and combined toe configurations illustrate the uncertainties involved in this kind of research as well as in the design and construction of dams.

It is evident that a purely external toe will not reduce pore pressures within the supporting rockfill. The study further documents the minor pore pressure increasing the effect of the external toe configuration. Although this results in marginal elevations of internal pore pressures, the overall mass slope stability is improved as documented by Morán and Toledo (2011). Perhaps the most significant feature of the external toe configuration would be the protective effect against erosion in the exit zone. Under extreme throughflow conditions, the high-intensity flow discharged at the small exit surface of the dam toe leads to concentration of streamlines. These destabilizing hydrodynamic forces coupled with the surface flow over the seepage exit face lead to progressive degradation of the surface of the dam slope, further resulting in unravelling deep-seated slides (Leps 1973). The external type toe helps stabilize the seepage exit zone under these circumstances thereby postponing damage to the main dam structure. Similar statements could be made regarding the combined toe configuration. The internal reach of the toe deals primarily with relieving the dam structure of pore-pressure build-up, whereas the external reach would act as a stabilizing agent in case of extreme throughflow or overflow scenarios.

At present times, the literature available on design methodology for dam toes for rockfill dams is scarce. Recent studies from Morán et al. (2019) present design guidelines and techniques for external toe protection for rockfill dams. However, no such methodologies are currently available for the design of internal or combined toe structures. Mishra and Parida (2006) and US Army Corps of Engineers (1993) present methodologies for design of toe structures and drainage blankets in earthfill dams. But this is of limited applicability for rockfill dams due to the very different material properties as well as a different geometry due to the slopes normally being much steeper in rockfill dams. The present investigation results yield relevant data in this regard, which can enable the progress towards well-defined design measures for rockfill dam toes. This in turn is intended at facilitating effective engineering decision-making with regards to ideal choice of rockfill dam toe design based on site-specific design restrictions.

Within this study, a change-point based statistical analysis has been employed for obtaining illustrative pore pressure measurements at different locations within the dam structure for incremental throughflow discharges. This methodology was found to be sophisticated considering its ability to automate the extraction of representative information from an extended time series with considerable variability. This facilitated description of hydraulic processes occurring within the dam structure. The methodology replaces what would otherwise be a manual extraction of representative values by visual observation of the data, a method which is more prone to errors and subjective bias. Further, the methodology could also have the potential for practical implementation in large scale constructions for automated safety monitoring of hydraulic structures. Employing time series of parameters such as leakage measurements, pore-pressure measurements, data sets of climatic indicators such as precipitation and temperature and so on could be employed to develop and further calibrate automated dam safety protocols. This could lead to more sophisticated warning systems for hydraulic structures.

Considering research applications, data sets accumulated as part of the experimental testing program could be further employed for validation of theoretical studies conducted in the past within the study discipline. Furthermore, the data sets could be valuable for calibration and validation of numerical models predicting throughflow behaviour in rockfill embankments. Permeability is an important input parameter for numerical modelling. Application of the data sets from the present study must consider that only the porosity of the materials is provided, since the permeability has not been measured directly. Enhancement of the capabilities of commercially available numerical seepage models should be of interest for researchers as well as for engineers and government agencies involved with rockfill dam design and safety assessment.

For any application of the research outcome, it must be kept in mind that the models presented herein are conceptual. Furthermore, that the study objective is to describe and compare the effects of the toe configurations on

throughflow hydraulic properties. These properties directly relate to the throughflow capacity of the dam in an overtopping situation, as well as pore pressure development in the downstream dam slope and thus to dam safety. Furthermore, it is not within the scope of the present study to provide configurations that are comparable in terms of practical issues such as cost or optimizing the dimensions of the toe structures. For this, further studies are required.

5.1. Recommendations for further studies

This study provides a small step forward in the field of investigating flow through rockfill dams, there are however significant knowledge gaps yet to be filled.

- Material properties such as permeability, porosity, density and anisotropy are important for understanding flow through and stability of rockfill dams. Further investigations are recommended in this regard to conduct model studies with different rockfill material.
- The rockfill shoulder material used in the present study was designed with a minimum grain size of 0.5 mm (equivalent to 5 mm in prototype) owing to lab restrictions. Further tests with a higher content of fine materials would be valuable as the amount of fines significantly affects the permeability of the material and thus the flow through the rockfill.
- Experimental tests were conducted as part of this study on rockfill dam models with steep downstream slope ($S = 0.67$). Conduction of similar investigations on rockfill embankments built at milder slopes is recommended to better understand the importance of embankment slope on throughflow development.
- Further experimental and numerical research is recommended to arrive at methodologies for optimal design of rockfill dam toes. Research considering calibration of the numerical models to the experimental data is ongoing at NTNU as a continuation of this experimental research.
- Study findings suggest that the crest section as a critical location for dam breach initiations in rockfill dams with unprotected downstream slopes. Further research is highly recommended in this regard to investigate measures for stabilization of rockfill dam crests.
- Throughflow tests within this study were conducted assuming overtopping of the dam core with steady-state flow conditions. However, during piping scenarios leading to entry of highly concentrated, turbulent throughflows into the dam structure, the rockfill dam structure could be subjected to much different throughflow conditions. Further investigations in this regard are highly recommended to study the behaviour of rockfill dams subjected to concentrated internal leakage situations.
- Carrying out large-scale field tests on rockfill dam structures are recommended to evaluate the validity of the findings at larger scales and to better understand the scale effects.

6. Concluding remarks

This article presents findings from experimental investigations conducted on 1:10 scale, 1 m high rockfill dam models built with well-graded rockfill material. The objective of this study was to investigate the hydraulic performance of three common rockfill dam toe types, external, internal and combined toes when subjected to throughflow scenarios. Data analysis was performed employing a change-point based statistical analysis which was found to provide a reliable and objective measure of arriving at representative flow and pore pressure values.

Investigation outcomes describe the effects of internal, external and combined toe configurations internal pore-pressure distributions within rockfill dam models subjected to throughflow conditions. Both the internal and combined toes were found to lead to significantly reduced pore-pressures within the dam structures as compared with rockfill dam models built with no toe. This in turn leads to increased slope stability in a high throughflow scenario, and also helps mitigate progressive toe damage. The external toe did not significantly affect the pore pressures within the dam, it did, however, significantly stabilize the toe section by preventing surface erosion.

The investigation results help advance the understanding of throughflow processes in rockfill dams and will hopefully provide insights that can lead to improved rockfill dam design. Considering research applications, data sets accumulated as part of the experimental testing program could be further employed for validation of theoretical studies conducted in the past within the study discipline. Furthermore, the data sets could be valuable for calibration and validation of numerical models predicting throughflow behaviour in rockfill embankments. Enhancement of capabilities of commercially available numerical seepage models should be of interest for researchers as well as for organizations involved with rockfill dam design and safety assessment. The data from these tests also illustrate how throughflow properties of a dam are governed not just by the composition of the material used but also the construction process adding to the uncertainties when analysing and designing rockfill dams. Furthermore, the change-point based statistical methodology could have potential for practical implementation in automated safety monitoring of hydraulic structures.

Notations

A	Area (m²)
A_d	Area of dam excluding core (m²)
B_b	Bottom width of dam (m)

B_t	Top width of dam (m)
$C_{u,S}$	Coefficient of uniformity of rockfill material (–)
$C_{u,T}$	Coefficient of uniformity of toe material (–)
$d_{50,S}$	Median particle size of rockfill material (m)
$d_{50,T}$	Median particle size of toe material (m)
H_d	Height of dam (m)
H_t	Height of toe structure (m)
L_d	Transverse length of dam (m)
m	number of samples (–)
N	number of discharge steps (–)
P	pore pressure (m)
Q	Pump capacity ($m^3\ s^{-1}$)
q_c	Critical unit discharge for breach initiation ($m^3\ s^{-1}$)
q_i	Unit discharge at i^{th} step ($m^3\ s^{-1}$)
S	Slope (V:H) of downstream embankment (–)
t	time (s)
x	pressure sensor number (–)
Δt	Time increment between discharge steps (s)
Δq	Incremental discharge step ($m^3\ s^{-1}$)
ρ_S	Density of rockfill material ($kg\ m^{-3}$)
ρ_T	Density of toe material ($kg\ m^{-3}$)

Acknowledgements

The authors acknowledge the financial support offered by HydroCen, Norway. The assistance offered by master students Mr Unnar Númi Almarsson and Mr Nils Solheim Smith is greatly appreciated.

Funding

This work was financially supported by the Norwegian Research Council [grant number 257588], Norwegian Research Centre for Hydropower Technology (HydroCen).

Notes on contributors

Geir H. Kiplesund holds an MSc degree in Civil and Environmental Engineering from the Norwegian University of Science and Technology (NTNU), Trondheim, Norway. He worked for Multiconsult ASA for 20 years as a consulting engineer, mainly on hydropower planning, dam safety, hydrology and hydraulics. He is currently a PhD candidate at the Department of Civil and Environmental Engineering at NTNU, Trondheim, Norway with research focus on stability and breaching of rockfill dams.

Ganesh H. R. Ravindra is a Project Manager on dams for Trondheim Municipality. He holds a PhD (2020) and MSc (2017) in Hydropower Development from the Norwegian University of Science and Technology (NTNU), Trondheim, Norway and a BE degree in Civil Engineering from MSRIT, Bangalore, India. He is currently a Project Manager on dam projects for Trondheim Municipality, Trondheim, Norway. His main research focus has been on rockfill dam stability under extreme loading conditions.

Marius M Rokstad Consulting Engineer, Asplan Viak, Trondheim. He holds a PhD (2016) and MSc (2012) in hydraulic and environmental engineering from NTNU. After graduating as a PhD he has worked as a Post Doc at NTNU. His main research areas has been on the use of statistical models for reliability and condition deterioration modelling of urban water systems' infrastructure, hydraulic modelling of pipe systems, risk analysis, and asset management of infrastructure systems.

Fjola G. Sigtryggsdottir is an Associate Professor at the Department of Civil and Environmental Engineering at NTNU. She graduated with a CS degree in civil engineering from the University of Iceland in 1993, and a master degree in structures and mechanics from the North Carolina State University in USA in 1994. She holds a PhD in geotechnical engineering from NTNU. She worked for Verkís Ltd (previously VST), Iceland, for 15 years as a consulting engineer, mainly on hydropower projects and rockfill dam design. Before joining NTNU, she was the Head of the Civil Engineering Department at the Reykjavík University, Iceland; as well as an independent consultant.

ORCID

Geir H. Kiplesund http://orcid.org/0000-0002-8574-840X
Ganesh H. R. Ravindra http://orcid.org/0000-0002-0351-0714
Marius M. Rokstad http://orcid.org/0000-0003-4650-3554
Fjóla G. Sigtryggsdóttir http://orcid.org/0000-0003-0428-8462

References

Abt SR, Johnson TL. 1991. Riprap design for overtopping flow. J Hydraul Eng. 117(8):959–972. DOI:10.1061/(ASCE)0733-9429(1991)117:8(959).

Chang HH. 1998. Riprap stability on steep slopes. Int J Sediment Res. 13:40–49.

Cruz PT, Materon B, Freitas M. 2009. Concrete face rockfill dams. São Paulo: CRC Press.

Dornack S. 2001. Uberstrombare Damme-Beitrag zur Bemessung von Deckwerken aus Bruchsteinen/ Overtopping dams-Design criteria for riprap.

Frizeii KH, Ruff JF, Mishra S. 1998. Simplified design guidelines for riprap subjected to overtopping flow. In Proceedings of the Annual Conference of the Association of State Dam Safety Officials. p. 301–312.

Hansen D, Garga VK, Townsend DR. 1995a. Flowthrough rockfill embankments: behavior in subzero temperatures. J Cold Reg Eng. 9(December):195–218. DOI:10.1061/(ASCE)0887-381X(1995)9:4(195).

Hansen D, Garga VK, Townsend DR. 1995b. Selection and application of a one-dimensional non-Darcy flow equation for two-dimensional flow through rockfill embankments. Canadian Geotechnical Journal. 32(2):223–232.

Hansen D, Roshanfekr A. 2012. Assessment of potential for seepage-induced unraveling failure of flow-through rockfill dams. Int J Geomech. 12(5):560–573. DOI:10.1061/(ASCE)GM.1943-5622.0000145.

Hansen D, Zhao WZ, Han SY. 2005. Hydraulic performance and stability of coarse rockfill deposits. Proc Inst Civ Eng: Water Manag. 158(4):163–175. DOI:10.1680/wama.2005.158.4.163.

Hiller PH. 2016. Kartlegging av plastring på nedstrøms skråning av fyllingsdammer. Trondheim: NTNU.

Hiller PH, Aberle J, Lia L. 2018. Displacements as failure origin of placed riprap on steep slopes. J Hydraul Res. 56(2):141–155. DOI:10.1080/00221686.2017.1323806.

Hiller PH, Lia L, Aberle J. 2019. Field and model tests of riprap on steep slopes exposed to overtopping. J Appl Water Eng Res. 7(2):103–117. DOI:10.1080/23249676.2018.1449675.

Hiller PH, Lia L, Aberle J, Wirtz S, Casper MC. 2009. Riprap design on the downstream slope of rockfill dams Laboratory test rig and "Smartstone" sensors. (2010), 1–6.

Hyllestad E, Andersen R, Østvold HM, Rystad V. 2012. Veileder for fyllingsdammer. 2018. Oslo: Norwegian Water Resources and Energy Administratinon. https://www.nve.no/Media/7086/veileder-med-rettelse-og-tilleggsnotat-juli-2018.pdf.

Javadi N, Mahdi TF. 2014. Experimental investigation into rockfill dam failure initiation by overtopping. Natl Hazards. 74(2):623–637. DOI:10.1007/s11069-014-1201-9.

Knauss J. 1979. Computation of maximum discharge at overflow rockfill dams (a comparison of different model test results). Technol Rev. 3:143–160.

Larese A, Rossi R, Oñate E, Toledo MÁ, Morán R, Campos H. 2015. Numerical and experimental study of overtopping and failure of rockfill dams. Int J Geomech. 15(4):04014060. DOI:10.1061/(ASCE) GM.1943-5622.0000345.

Larsen P, Bernhart HH, Schenk E, Blinde A, Brauns J, Degen FP. 1986. Uberstrombare Damme, Hochwasserentlastung uber Dammscharten/ Overtoppable dams, spillways over dam notches. Unpublished Report Prepared for Regierungsprasidium Karlsruhe, Universita.

Leps TM. 1973. Flow through rockfill. In: Poulos SJ, Hirschfeld RC, editors. Embankment-dam engineering. Vol. 12. New York: John Wiley and Sons INC.

Leps TM. 1979. CHAPTER 2 - Flow Through Rockfill. In: Stephenson David, editor. *Rockfill in hydraulic engineering*. Vol. 27. Elsevier; p. 19–37. https://doi.org/10.1016/B978-0-444-41828-9.50007-7.

Lev V, Anantharamu V. 2020. Estimating the elastic properties of mica and clay minerals. Geophysics. 85(2):MR83–MR95.

Marulanda A, Pinto N L de S. 2000. Recent experience on design, construction, and performance of CFRD dams. In: *Concrete face rockfill dams*. Beijing: Barry Cooke; p. 279–299.

Mishra GC, Parida B. 2006. Earth dam with toe drain on an impervious base. Int J Geomech. 6:379–388.

Morán R. 2015. Review of embankment dam protections and a design methodology for downstream rockfill toes. Dam Protections against overtopping and accidental leakage – proceedings of the 1st international seminar on dam protections against overtopping and accidental leakage. p. 25–39.

Morán R, Toledo MÁ. 2011. Research into protection of rockfill dams from overtopping using rockfill downstream toes. Can J Civ Eng. 38(12):1314–1326. DOI:10.1139/L11-091.

Morán R, Toledo MÁ, Larese A, Monteiro-Alves R. 2019. A procedure to design toe protections for rock fill dams against extreme through- flows. Eng Struct. 195(May):400–412. DOI:10.1016/j.engstruct.2019.06.004.

NTNU. 2020. Course Compendium for VM6001- Dam Safety. Trondheim: Department of Civil and Environmental Engineering, NTNU.

Olivier H. 1967. Through and overflow rockfill dams-New design techniques. Proc Inst Civ Eng. 36(3):433–471. https://doi.org/10.1680/iicep.1967.8530.

Peirson WL, Figlus J, Pells SE, Cox RJ. 2008. Placed rock as protection against erosion by flow down steep slopes. Journal of Hydraulic Engineering. 134(9):1370–1375. DOI:10.1061/(ASCE)0733-9429(2008)134:9(1370).

Ravindra GHR. 2020. Hydraulic and structural evaluation of rockfill dam behavior when exposed to throughflow and overtopping scenarios (Nowegian University of Science and Technology). https://ntnuopen.ntnu.no/ntnu-xmlui/handle/11250/2670688.

Ravindra GHR, Gronz O, Dost B, Sigtryggsdóttir FG. 2020. Description of failure mechanism in placed riprap on steep slope with unsupported toe using smartstone probes. Eng Struct. 221:111038. DOI:10.1016/j.engstruct.2020.111038.

Ravindra GHR, Sigtryggsdóttir FG, Høydal ØA. 2019. Nonlinear flow through rockfill embankments. J Appl Water Eng Res. 7(4):247–262. DOI:10.1080/23249676.2019.1683085.

Ravindra GHR, Sigtryggsdottir FG, Lia L. 2018. Protection of embankment dam toe and abutments under overtopping conditions. 3rd International Conference on Protection against Overtopping, (June), 6–8.

Siddiqua S, Blatz JA, Privat NC. 2013. Evaluating the behaviour of instrumented prototype rockfill dams. Can Geotech Jl. 50(3):298–310. DOI:10.1139/cgj-2011-0371.

Solvik O. 1991. Throughflow and stability problems in rockfill dams exposed to exceptional loads. Sixteenth International Congress on Large Dams. 333–343.

Sommer P. 1997. Uberstrombare Deckwerke/ Overtoppable erosion protections. Unpublished Report No. DFG-Forschungsbericht La 529/8-1, Universita.

Toledo MÁ, Moran R, Onate E. 2015. Dam protections against overtopping and accidental leakage. In Dam Protections against overtopping and accidental leakage. https://doi.org/10.1201/b18292.

Townsend RD, Garga VK, Hansen D. 1991. Finite difference modelling of the variation in piezometric head within a rockfill embankment. Can J Civ Eng. 18(2):254–263. DOI:10.1139/l91-030.

US Army Corps of Engineers. 1993. *Seepage analysis and control for dams*.

USDA. 2017. Chapter 26. Gradation design of sand and gravel. In: National Engineering Handbook Part 633. Washington, DC: US Department of Agriculture.

Worman A. 1993. Seepage induced mass wasting on coarse soil slopes. Journal of Hydraulic Engineering. *119*(10):1155–1168.